

## **STUDY OF TANTALUM SUBSTITUTED POTASSIUM TUNGSTEN BRONZES**

MD. MAHBUBUR R. SHAKIL<sup>a#</sup>, TAPAS DEBNATH<sup>a\*</sup>, CLAUD H. RÜSCHER<sup>b</sup> AND ALTAF HUSSAIN<sup>a,c</sup>

<sup>a</sup>*Department of Chemistry, University of Dhaka, Dhaka-1000, Bangladesh*

<sup>b</sup>*Institute for Mineralogy, Leibniz University of Hannover, Callinstr. 3, D- 30167 Hannover, Germany*

<sup>c</sup>*Centre for Advanced Research in Sciences, University of Dhaka, Dhaka-1000, Bangladesh*

### **Abstract**

A series of compounds  $K_xTa_yW_{1-y}O_3$  with  $x = 0.30, 0.00 \leq y \leq 0.30$  and  $x = 0.55, 0.00 \leq y \leq 0.10$  were synthesized by conventional solid-state method. The samples were characterized using XRD and FTIR spectroscopy. X-ray powder patterns reveal that the samples with compositions  $x = 0.30, y \leq 0.30$  show hexagonal tungsten bronze (HTB) type phase and the samples with  $x = 0.55, 0.02 \leq y \leq 0.10$  show a mixture of two phases (K-HTB and tetragonal potassium tungsten bronze, K-TTB). The samples of the system,  $K_{0.30}Ta_yW_{1-y}O_3$  with  $0.00 \leq y \leq 0.15$  shows no significant change in the cell parameters. However, for the composition  $y > 0.15$ , the cell parameter  $a$  decreases and  $c$  increases with increasing Ta content, which may be explained by the ordering of Ta for  $y > 0.15$  suggesting the transformation to another space group. The appearance of absorption peak in the infrared absorption spectra of  $K_{0.3}Ta_yW_{1-y}O_3, y > 0.10$  samples indicate the transition to non-metallic phase.

### **Introduction**

The tungsten bronzes are well known as non-stoichiometric compounds of general formula  $A_xWO_3$  where A is typically an electropositive element such as an alkali, alkaline earth or a rare earth metal and  $x$  varies between 0 and 1. All tungsten bronzes structure,  $A_xWO_3$ , can be described as the host structure of tungsten (VI) oxide,  $WO_3$ , into which A atoms have been introduced interstitially. The structure of these compounds is greatly influenced by the amount of inserted electropositive metal atom, A and the synthesis temperature. There are four types of structurally different tungsten bronzes has been reported so far namely Perovskite Tungsten Bronzes (PTB), Tetragonal Tungsten Bronzes (TTB), Hexagonal Tungsten Bronzes (HTB), and Intergrowth Tungsten Bronzes (ITB)<sup>1-6</sup>. The structure of hexagonal tungsten bronze can be described as a three dimensional network of corner sharing  $WO_6$  octahedra containing hexagonal and trigonal tunnel along  $c$  axis (Fig. 1). The metal ions, A, occupy only the hexagonal tunnels. The homogeneity range of HTB for  $A_xWO_3$  with  $A=K, Rb, Cs$  is found to be  $0.19 \leq x \leq 0.33$ <sup>7</sup>. However, this lower stability limit greatly depends on preparation conditions and can be

---

\*Author for Correspondence; email: [debnath@univdhaka.edu](mailto:debnath@univdhaka.edu), # Present address: Department of Chemistry, Dhaka University of Engineering & Technology, Gazipur-1700

extended up to  $x = 0.15$ . The upper stability limit of HTB phase ( $x = 0.33$ ) corresponds to the sites available for metal ion A within the hexagonal tunnel.

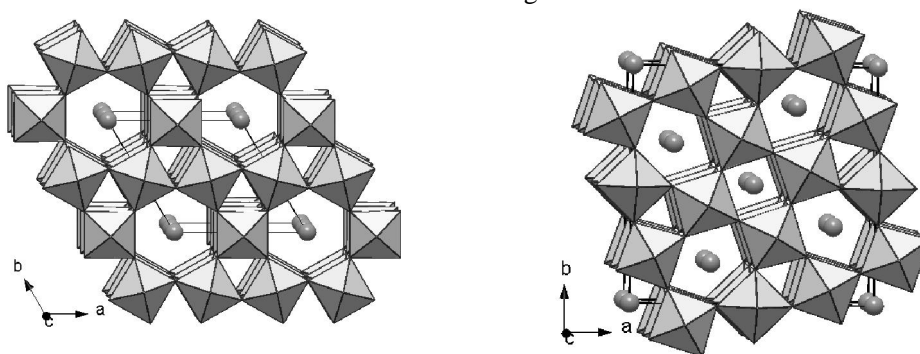


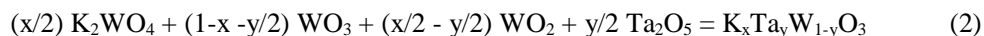
**Fig. 1.** Structural model of Hexagonal Tungsten Bronze, HTB (left) and Tetragonal Tungsten Bronze, TTB (right).

Similar to HTB, TTB can be regarded as corner sharing of  $WO_6$  octahedra forming three types of tunnels, namely trigonal, tetragonal and pentagonal. The A ions can be located either in the tetragonal or pentagonal tunnels but most of the metal ions show a preference for the larger size pentavalent tunnels as shown in Fig. 1. In 1976, Takusagawa and Jacobsson<sup>8</sup> reported that with increasing the alkali metal content the pentagonal tunnels are filled first and then tetragonal tunnels. This may be due to the fact that the pentagonal tunnels have more available space than those of tetragonal tunnels and therefore large cation favors the pentagonal tunnels first.

Tungsten bronzes and substituted tungsten bronzes<sup>9-11</sup> have been studied extensively because of their interesting physical and chemical properties. Tungsten bronzes,  $A_xWO_3$  can also be written as  $A_xW^{5+}_yW^{6+}_{1-y}O_3$ , which indicates the presence of pentavalent tungsten ions in it. Literature survey shows that the pentavalent tungsten ions can be partially (i.e. when  $x > y$ ) or fully substituted (i.e. when  $x = y$ ) by other ions<sup>12-18</sup>. Fully substituted phase analogue to ITB is called bronzoid<sup>19</sup>. Deschanvres et al.<sup>20</sup> studied bronzoid type phase of tantalum substituted series. However, there is no systematic study on Ta substituted K-HTB and K-TTB. This has incited us to do a systematic study on tantalum substituted potassium tungsten bronzes.

### Experimental

Powder samples of the system  $K_xTa_yW_{1-y}O_3$  with  $x = 0.30, 0.0 \leq y \leq 0.30$  and  $x = 0.55, 0.0 \leq y \leq 0.10$  have been prepared from appropriate mixture of  $K_2WO_4$ ,  $WO_3$ ,  $WO_2$  and  $Ta_2O_5$  by conventional solid state synthesis method at  $800^\circ C$ .



Starting materials were high quality reagent grade chemicals  $\text{WO}_2$  (99.9 % Pure, Alfa Aesar),  $\text{WO}_3$  (Herman Strack),  $\text{Ta}_2\text{O}_5$  (Strem Chemical).  $\text{K}_2\text{WO}_4$  was prepared by heating equimolar mixtures of  $\text{K}_2\text{CO}_3$  (99.95%, Alfa Aesar) and  $\text{WO}_3$  (Eqn. 1) in air at  $600^\circ\text{C}$  for 4 days. The purity of all reactants was checked by taking X-ray powder patterns.

The reactants mixtures with appropriate molar ratio (Eqn. 2) were mechanically mixed in an agate mortar which were then put in a silica glass tube and then evacuated ( $10^{-2}$  torr) and sealed. The sealed tubes were heated in a muffle furnace at  $800^\circ\text{C}$  for 7 days. The products were characterized by XRD using Guinier-Hägg focusing camera with  $\text{Cu K } \alpha_1$  radiation ( $\lambda = 1.540598\text{Å}$ ) and silicon, Si ( $a = 5.43088\text{ Å}$ ) was added as an internal standard. The X-ray films were evaluated with a computerized film scanner (Line scanner LS 20) and the unit cell parameters were refined by using the programs SCANPI<sup>21</sup> and PIRUM<sup>22</sup>. Besides, the XRD patterns of selected samples of HTB series were collected using  $\text{CuK } \alpha$  radiation in a Phillips PV-1800 diffractometer to verify the results obtained from X-ray film method. The hkl fit was done using Rietveld program, TOPAS.

Infrared absorption spectra of samples,  $\text{K}_{0.30}\text{Ta}_y\text{W}_{1-y}\text{O}_3$ , were investigated by a FTIR spectrometer (Bruker IFS66v) within the range  $370\text{-}4000\text{ cm}^{-1}$ . The finely ground samples were mixed with KBr (1.0 mg sample with 200.0 mg KBr) and pressed into pallets of 13 mm diameter to measure transmission IR. The spectra are shown in the absorption units  $\text{Abs} = \log(I_0/I)$ , where  $I_0$  and  $I$  are transmitted intensities through the reference pellet (KBr) and sample pellet diluted with KBr, respectively.

## Results and Discussion

### HTB system

X-ray powder patterns of  $\text{K}_{0.30}\text{Ta}_y\text{W}_{1-y}\text{O}_3$  samples are shown in Fig. 2.

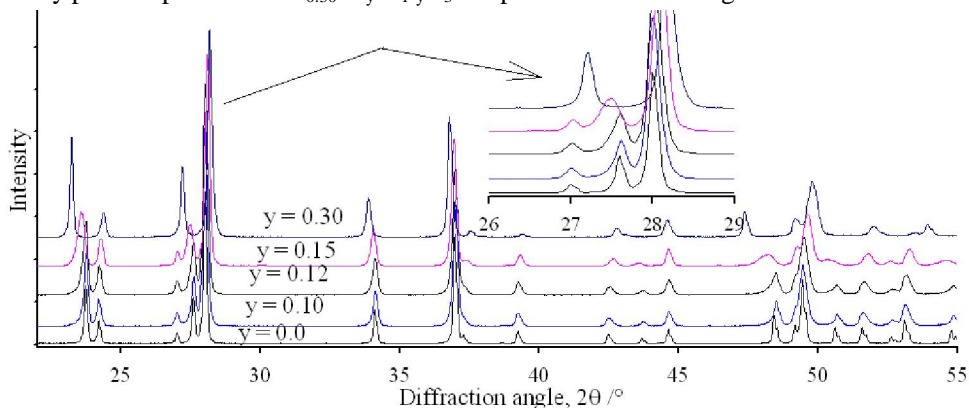


**Fig. 2.** X-ray diffraction patterns of some selected samples with nominal compositions  $\text{K}_{0.3}\text{Ta}_y\text{W}_{1-y}\text{O}_3$ . An enlarge view (inset) shows that the number of diffraction peaks for certain planes are systematically decreasing with increasing Ta content. The patterns are shifted vertically for the sake of clarity.

All diffraction peaks could be indexed as HTB type phase. A careful observation of the X-ray powder patterns reveal that the number of lines in the system  $K_{0.30}Ta_yW_{1-y}O_3$  decreases systematically (inset of Fig. 2) with the increasing nominal tantalum content. This systemic disappearance of weak lines may be due to different scattering factor of tantalum ions as well as due to the statistical distribution of the  $Ta^{5+}$  ions for high Ta content samples. The statistical distribution reveals the possibility of being a different space group, which, however, was not considered in the present study. In this study, space group Pbam was used for the hkl fit (Fig. 3).

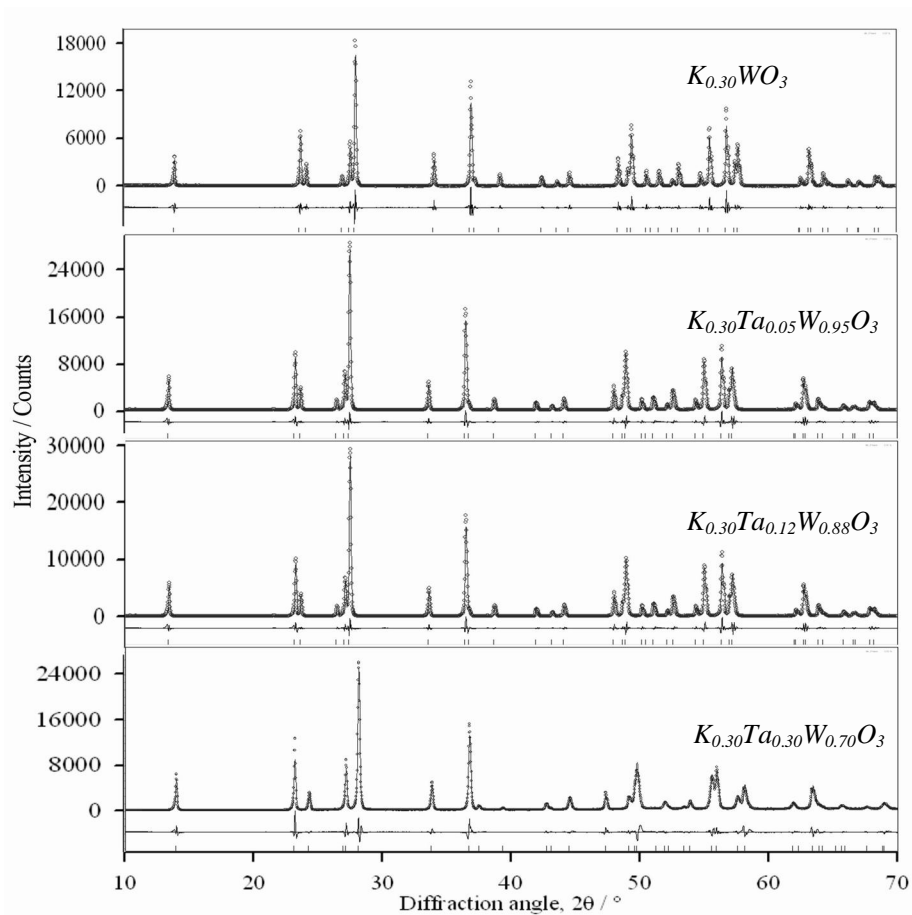


**Fig. 3.** hkl refinement fit of some selected samples of  $K_{0.3}Ta_yW_{1-y}O_3$  series. The dots, line through the dots and curve above the bars represent the observed, calculated and difference XRD patterns, respectively. The positions of the diffraction peaks are shown by bar.

The cell parameters of the system,  $K_{0.30}Ta_yW_{1-y}O_3$  (Table 1) show the cell parameters of  $y = 0.0$  sample prepared in this study agrees well with the previously reported values<sup>12</sup>. Additionally, the cell parameters are plotted as a function of nominal Ta content (Fig. 4), showing both of the cell parameters,  $a$  and  $c$  do not change significantly upto  $y = 0.15$ . Hussain et al.<sup>12</sup>, however, reported that in the Nb substituted HTB type  $K_{0.30}Nb_yW_{1-y}O_3$  system both of the cell constants  $a$  and  $c$  decreases with increasing Nb content, which may be comparable with cubic  $Li_xWO_3$  system where cell parameters decrease due to the tilting of  $WO_6$  octahedra.

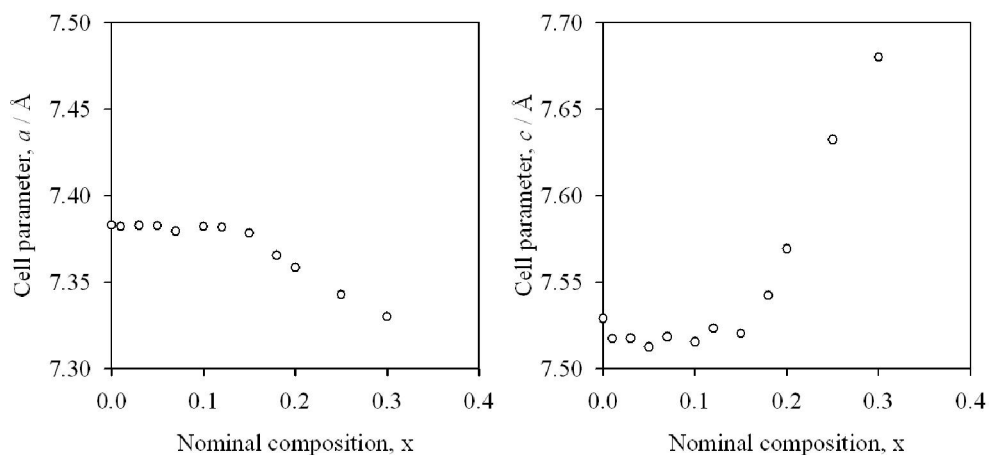


**Fig. 4.** Variation of lattice parameters ( $a$  and  $c$ ) of HTB as a function of nominal tantalum content. Both of the lattice parameters remain constant up to certain Ta content then changes significantly.

In the present case, the cell parameters remain constant up to  $y = 0.15$ , which may implies less effect on the tilting of the  $WO_6$  octahedra on Ta doping. On the other hand the cell parameter  $a$  rapidly decreases while  $c$  increases for  $y > 0.15$ , which may be explained by the ordering of Ta for  $y > 0.15$  suggesting the transformation to another space group.

The IR absorption spectra of the system,  $K_{0.30}Ta_yW_{1-y}O_3$  are shown in the Fig. 5. The spectrum of tantalum free HTB phase has weak broad phonon absorption band below  $1000\text{ cm}^{-1}$  which is related to air oxidation of surface of the sample. The effect of IR active phonon absorption becomes usually further small in metallic conducting system with effective free carrier plasma frequencies above the phonon absorption frequency. The absorption feature as a function of  $y$  shows a significant increase of its intensity for  $y > 0.10$ . Therefore, the increased phonon absorption intensity for  $y > 0.10$  indicates a significant decrease in the free carrier contribution and results nonmetallic nature of the compounds. The spectra observed for the sample  $K_{0.30}Ta_yW_{1-y}O_3$  are in good agreement with powder related spectra reported by Dey et al.<sup>15</sup> recently.

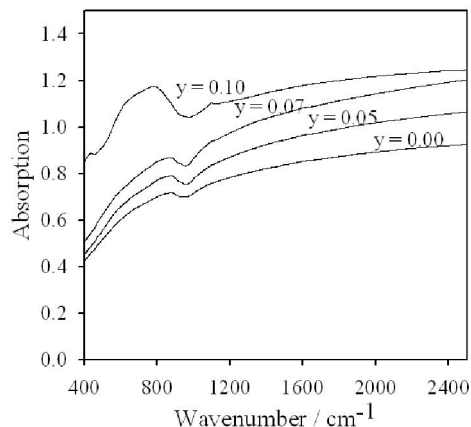


**Fig. 5.** IR absorption spectra of some of the selected samples of HTB phases showing phonon absorption peak(s) for  $y = 0.10$  sample, which indicates the transformation from metallic to non-metallic character due to the Ta doping (i.e. counter doping effect).

#### TTB system

X-ray powder patterns of  $K_{0.55}Ta_yW_{1-y}O_3$  are shown in Fig. 6. The sample of  $K_{0.55}Ta_yW_{1-y}O_3$  with  $x = 0.55$ ,  $0.02 < y < 0.10$ , shows TTB phase along with an additional phase, which could be indexed as HTB phase. It is important to note that the appearance of HTB phase increases with the nominal composition of Ta. Some weak reflections were also observed specifically for the case of  $K_{0.55}Ta_yW_{1-y}O_3$  with  $y = 0.10$ , which could not be indexed.

The cell parameters for pure TTB phase with  $x = 0.55$  differ slightly from the reported data<sup>7</sup>. This little deviation of cell parameters may be due to the difference of nominal and actual composition. This presumption has been confirmed when the corresponding composition for observed cell dimensions was determined from the reported<sup>23</sup> cell parameter-composition plot. It is found that the experimentally observed cell parameter corresponds to  $x = 0.42$  rather than  $x = 0.55$ .

**Table 1.** Lattice parameters of  $K_xTa_yW_{1-y}O_3$  prepared by conventional solid state method at  $800^\circ\text{C}$ .

Nominal composition $K_xTa_yW_{1-y}O_3$	Cell Parameters		
	$a(\text{ \AA})$	$c(\text{ \AA})$	
$x = 0.30$ (HTB)	$y = 0.00$	7.3829(3)	7.5290(5)
	$y = 0.01$	7.3823(7)	7.517(1)
	$y = 0.03$	7.3828(4)	7.5175(6)
	$y = 0.05$	7.3825(7)	7.512(1)
	$y = 0.07$	7.3794(7)	7.518(1)
	$y = 0.10$	7.3822(4)	7.5154(9)
	$y = 0.12$	7.3818(9)	7.523(1)
	$y = 0.15$	7.3785(9)	7.520(1)
	$y = 0.18$	7.3655(9)	7.542(2)
	$y = 0.20$	7.358(1)	7.569(2)
$x = 0.55$ (TTB)	$y = 0.00$	12.259(1)	3.8256(1)
	$y = 0.02$	12.289(1)	3.8319(6)
	$y = 0.05$	12.300(2)	3.8354(9)
	$y = 0.08$	12.283(1)	3.833(1)
	$y = 0.10$	12.293(1)	3.8361(9)

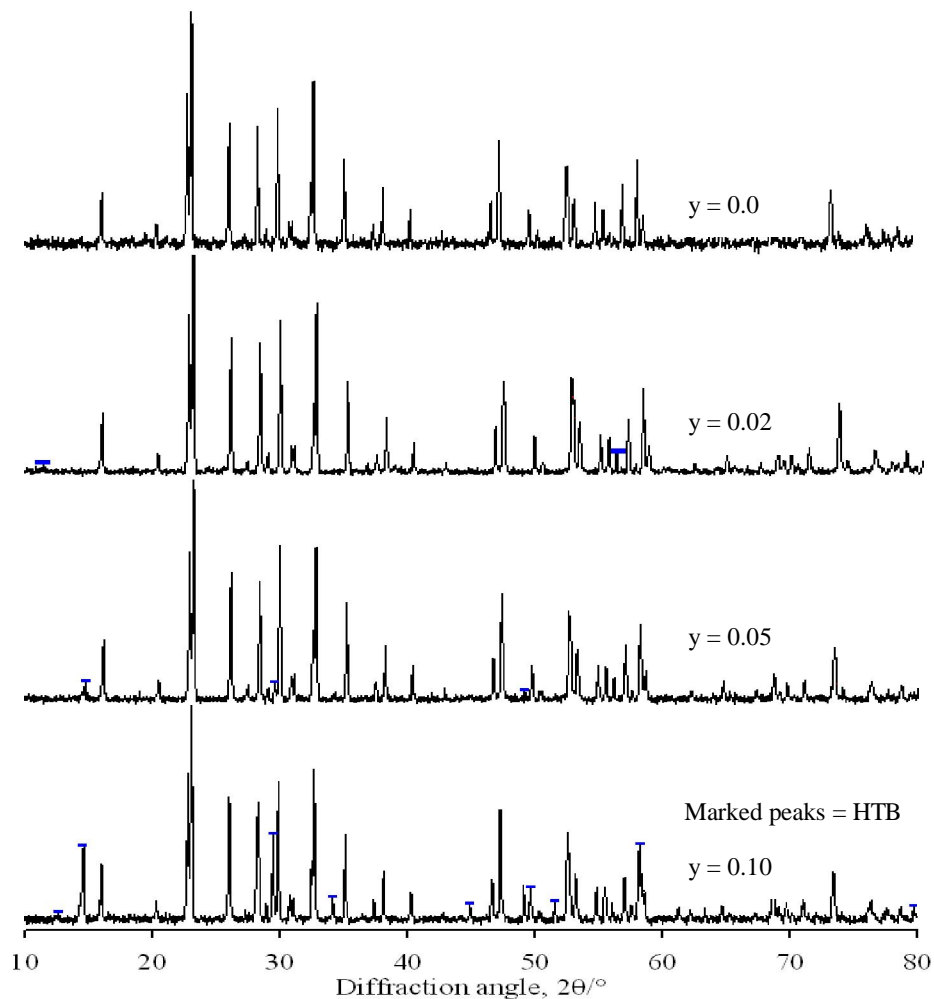


**Fig. 6.** X-ray powder patterns of some selected samples (TTB) with nominal compositions  $K_{0.55}Ta_yW_{1-y}O_3$ . Si was added as an internal standard. Additional phase(s) appear with increasing Ta content.

### Conclusion

Hexagonal and tetragonal potassium tungsten bronzes,  $K_xWO_3$ , and their tantalum-substituted forms,  $K_xTa_yW_{1-y}O_3$ , have been prepared by conventional solid-state synthesis method at  $800^\circ\text{C}$ . The XRD data of the samples show that the pure HTB type phase could be prepared for  $x = 0.30$ , and  $y = 0.30$ . The samples of the system,  $K_{0.30}Ta_yW_{1-y}O_3$  with nominal  $0.00 \leq y \leq 0.15$  shows no significant change in the cell parameters.

However, for the nominal composition  $y > 0.15$ , the cell parameter  $a$  decreases and  $c$  increases with increasing Ta content, which may be explained by the ordering of Ta for  $y > 0.15$  suggesting the transformation to another space group. The appearance of absorption peak in the infrared absorption spectra of  $K_{0.3}Ta_yW_{1-y}O_3$ ,  $y > 0.10$  samples indicate the transition to non-metallic. In the system,  $K_{0.55}Ta_yW_{1-y}O_3$  with  $0.02 < y < 0.10$ , a mixture of tantalum substituted K-HTB and K-TTB phases formed.

### Acknowledgement

The authors gratefully acknowledge the Ministry of Science and Information & Communication Technology, Government of Bangladesh and Alexander von Humboldt foundation, Germany, for financial supports.

### References

1. G. Hägg, *Z. Physik. Chem.*, 1935, **B29**, 192.
2. A. Magneli *Arkiv. kemi.*, 1949, **1**, 213.
3. A. Magneli, *Acta Chem. Scand.*, 1951, **5**, 670.
4. A. Magneli, *Acta Chem. Scand.*, 1953, **7**, 315.
5. P.G. Dickens and M.S. Whittingham, *Quart. Rev. Chem. Soc.*, 1968, **22**, 30.
6. A. Hussain and L. Kihlberg, *Acta Crystallogr.*, 1976, **A32**, 551.
7. A. Hussain, *Chem. Commun. Univ. Stockholm*, 1978, **2**, 1.
8. F. Takusagawa and R. A. Jacobson, *J. Solid State Chem.*, 1976, **18**, 163.
9. L. H. Cadwell, R.C. Morris and W.G. Moulton, *Phys. Rev.* 1981, **B23**, 2219.
10. R. Brusetti, P. Bordet and J. Marcus, *J. Solid State Chem.*, 2003, **172**, 148.
11. J. Gou, C. Dong, L. Yang and H. Chen, *Mater. Res. Bull.*, 2008, **43**, 779.
12. A. Hussain, A. Ul-Monir, M.M. Murshed and C.H. Rüschler, *Z. Anorg. Allg. Chem.*, 2002, **628**, 416.
13. T. Debnath, C.H. Rüschler, Th. M. Gesing, J. Koepke and A. Hussain, *J. Solid State Chem.*, 2008, **181**, 783.
14. T. Debnath, S.C. Roy, C.H. Rüschler and A. Hussain, *J. Mater. Sci.*, 2009, **44**, 179.
15. K.R. Dey, T. Debnath, C. H. Rüschler, M. Sundberg and A. Hussain, *J. Mater. Sci.*, 2010, **46**, 1388.
16. R. Sharma, *Mater. Res. Bull.*, 1985, **20**, 1373.
17. Y. Miyamoto, S. Kume, J. P. Doumerc and P. Hagenmuller, *Mater. Res. Bull.*, 1983, **18**, 1463.
18. M. A. Dubson and D.F. Holcomb, *Phys. Rev.*, 1985, **B32**, 1955.
19. A. Magnéli, *12<sup>th</sup> European Crystallographic Meeting, Moscow*, 1989.
20. A. Deschanvres, M. Frey, B. Raveau and J.c. Thomazea, *Bull. Soc. Chim. Fr*, 1968, **9**, 3519.
21. K. –E. Johanson, T. Plam and P. –E. Werner. *J. Phys.*, 1980, **E13**, 1289.
22. P. –E. Werner, *Ark. Kemi*, 1969, **31**, 513.
23. A. Hussain and L. Kihlberg, *Analytica Chemica Acta*, 1977, **90**, 283.

(Received: 26 December, 2011; Accepted : 4 April, 2012)